Construction and Building Materials 229 (2019) 116885

Contents lists available at ScienceDirect

Construction and Building Materials

journal homepage: www.elsevier.com/locate/conbuildmat

Microalga-induced biocementation of martian regolith simulant: Effects of biogrouting methods and calcium sources

Jason Gleaton [a], Zhengshou Lai [b], Rui Xiao [a], Qiushi Chen [c], Yi Zheng [a,*]

[a] Department of Environmental Engineering and Earth Sciences, Clemson University, 342 Computer Court, Anderson, SC 29625, USA
[b] School of Intelligent Systems Engineering, Sun Yat-sen University, Guangzhou 510275, China
[c] Department of Civil Engineering, Clemson University, 320 Lowry Hall, Clemson, SC 29634, USA

HIGHLIGHTS

- Microalga *Thraustochytrium striatum* was studied for biocementation of Martian Regolith Simulant (MRS).
- *T. striatum* can induce biocementation in the presence of urea and $CaCl_2$.
- Biogrouting method had significant effect on the properties of biocemented MRS columns.
- Calcium acetate is a potential alternative calcium and carbon sources for biocementation to $CaCl_2$.
- Calcium acetate achieved 95% reduction of hydraulic conductivity compared to untreated MRS.

ARTICLE INFO

Article history:
Received 18 January 2019
Received in revised form 11 August 2019
Accepted 4 September 2019
Available online 10 September 2019

Keywords:
Biocementation
Biogrout
Martian regolith simulant
Anaerobic digestion
Thraustochytrium striatum
Unconfined compressional strength
Hydraulic conductivity

ABSTRACT

A microalga, *Thraustochytrium striatum* was studied for biocementation of Martian regolith simulant (MRS). Calcium acetate derived from simulated anaerobic digestion (AD) was tested to replace $CaCl_2$ for making biocement. Biogrouting methods, calcium salt/urea molar ratios, and alternative calcium salt were investigated on biocementation with *T. striatum*. Of biogrouting methods, batch feeding produced columns with maximum unconfined compressional strength of 732 kPa while reducing hydraulic conductivity over 50% compared to the untreated MRS. The simulated AD-derived calcium acetate induced $CaCO_3$ precipitate in biocementation. With *T. striatum*, calcium acetate could serve as carbon and calcium sources to generate $CaCO_3$ precipitate without urea.

1. Introduction

Biocementation, also known as microbially induced carbonate precipitation (MICP), involves the use of microorganisms to precipitate calcium carbonate ($CaCO_3$) as a binding agent for a novel eco-friendly alternative to conventional construction materials [1–4]. Over the last decade scientist have conducted studies on the novel idea of utilizing MICP microorganisms to repair damaged concrete structures, improve soil stabilization, and to replace conventional cement production [4–7]. Biocementation has proven in lab-scale experiments to improve the mechanical properties and reduce hydraulic conductivity, producing a similar material comparable to cement utilizing sand and MICP microorganisms [3,4,6–9]. Though biocementation has proven to be a viable alternative, currently the utilization of the process outside of lab-scale experiments is still difficult. The utilization of biocementation is costly due to the amount of nutrients needed to cultivate the microbes and facilitate the precipitation of $CaCO_3$ [10,11]. Excluding the high costs of biocementation, the process has the potential to have both harmful effects to current infrastructure and the surrounding environment [3,4,6,7,11]. Despite the unfavorable situation, biocementation is still a potential eco-friendly alternative to conventional cement with continuous research on how to improve the process and reduce its negative effects.

The formation of $CaCO_3$ is affected by many factors, such as the microorganism, concentration/source of calcium, dissolved inorganic carbon, pH of the system, and the amount of available nucleation sites [3,10,12]. The method of biogrouting has an effect on

* Corresponding author at: Department of Grain Science and Industry, Kansas State University, 101C BIVAP, 1980 Kimball Avenue, Manhattan, KS 66506, USA.
E-mail address: yzheng@ksu.edu (Y. Zheng).

https://doi.org/10.1016/j.conbuildmat.2019.116885
0950-0618/

the localization of the precipitated $CaCO_3$, which effects the strength of produced biocement [3,13,14]. There are two main methods of biogrouting, which are the injection and premixing methods [3,5]. The main difference between these two methods is how the microorganisms are added to the regolith. The injection method typically involves adding the microorganism onto the top of the regolith within a reactor and allowing it to flow through the regolith [3,5]. While the premixing method involves physically mixing the microorganisms with the regolith before adding the regolith into a reactor [3,5]. The types of microorganisms that are involved in MICP include photosynthetic organisms, sulfate-reducing bacteria, and some organisms that utilize nitrogen cycle [3,15,16]. The most widely studied biocementation microorganisms (e.g., *Sporosarcina pasteurii*) are urease-producing bacteria (UPB) that use nitrogen cycle, more specifically urea hydrolysis to generate $CaCO_3$ [12,16-18]. The UPB can create biocement in the presence of calcium and urea according to the stoichiometry of $CO(NH_2)_2 + 2H_2O + Ca^{2+} \overset{UPB}{\rightarrow} CaCO_3 \downarrow + 2NH_4^+$ through urea hydrolysis by urease produced by the UPB (Fig. 1), during which $CaCO_3$ precipitate is generated associated with ammonia emission due to the pH increase to basic level.

The motivation of this research is to develop an earth-independent biocementation process to produce biocemented construction materials for space applications (e.g., Mars exploration). However, many challenges (e.g., biocementation microorganisms and calcium sources) need to be addressed before biocementation technology can be adopted for self-sustaining space exploration missions. First of all, we need to find robust biocementation microorganisms that could survive under the Martian environment (e.g., CO_2-dominant atmosphere and temperature variation) because the common biocementation UPB on Earth are aerobic and grow under proper temperature (e.g., room temperature) so that they may not be able to grow on Mars. Given the special environmental conditions on Mars, some microalgae may be suitable for biocementation on Mars owing to their photosynthesis capability and adaptation to a wide range of temperature. Secondly, the commonly used calcium salt $CaCl_2$ is expensive and would not be available on Mars. Therefore, we need to find cheap and abundant alternative calcium sources for biocementation. A process such as anaerobic digestion (AD) could fulfill the needs of producing alternative calcium salts using *in-situ* Martian resources. In AD, organic matter can be degraded into volatile fatty acids (VFAs) which are then converted into methane for energy production [20,21]. We can manipulate the AD process to halt it at the VFAs production stage and use the VFAs (mainly in acetate) to dissolve $CaCO_3$-rich limestone or Martian rocks to produce soluble calcium salts (e.g., calcium acetate) which could be used for the MICP process for biocementation on Mars [4,11].

In this research, we studied an unprecedentedly used microalga, *Thraustochytrium striatum* as a representative potential biocementation microorganism because it can grow on both urea and acetate to produce carbonate through both urea hydrolysis and acetate metabolism, respectively [22]. The ammonia emission that is an intrinsic issue of the conventional UPB-induced biocementation could be eliminated when *T. striatum* is used for biocementation with acetate as a carbon source. Therefore, we compared urea with acetate for biocementation with *T. striatum*. An additional potential benefit of *T. striatum* is it can tolerate temperature variation. To study the feasibility of using AD process to produce soluble calcium source from Martian rocks, we used acetic acid (to simulate acetate-rich VFAs) and limestone (to simulate Martian rocks) [4,11] to make simulated AD-based calcium acetate which was then used for biocementation of Martian regolith simulant (MRS) (to simulate Martian soil) with *T. striatum*. In doing so, we would expect to avoid ammonia emission during biocementation by using *T. striatum* while saving cost from no need of urea. The specific objectives of this research were to: (1) study the *T. striatum*-specific biogrouting methods for manufacturing biocemented MRS columns; (2) investigate the effect of $CaCl_2$/urea molar ratio on the unconfined compressional strength (UCS) and hydraulic conductivity of biocemented MRS columns; and (3) utilize simulated AD-based calcium acetate as a calcium/carbon source to make biocemented MRS columns with *T. striatum*.

2. Materials and methods

2.1. Thraustochytrium striatum culture and MRS preparation

The microorganism used for biocementation in this research was *T. striatum* ATCC 24473 which was purchased from the American Type Culture Collection (ATCC). The stock and seed cultures were prepared by following the protocols provided by ATCC. Briefly, *T. striatum* was sub-cultured every 7 days and maintained on an artificial sea water (ASW) agar medium plate made of ASW, glucose, yeast extract, peptone, and agar. The ASW contained (g/L): 30.0 NaCl, 0.7 KCl, 10.8 $MgCl_2 \cdot 6H_2O$, 5.4 $MgSO_4 \cdot 7H_2O$, and 1.0 $CaCl_2 \cdot 2H_2O$. The concentrations of glucose, yeast extract, peptone, and agar were 30.0, 6.0, 6.0, and 10 g/L, respectively. After the chemicals were dissolved into 1.0 L of deionized distilled (DDI) water, the pH of the broth was adjusted to pH 7.0 using 1 M NaOH followed by autoclave at 121 °C for 15 min. The inoculum was cultivated in 500-mL flasks with 100 mL working volume to which 10 mL seed culture (obtained at mid-log phase of seed culture preparation) was inoculated (1:10, v/v inoculation size) into the fresh broth and incubated at 25 °C with a stirring speed of 140 rpm. After 7 days of cultivation, *T. striatum* cells were harvested by centrifugation and re-suspended in DDI water to make cell "solution" for biocementation.

The MRS used in this research was the Mojave Mars Simulant, which was developed using a basalt mined in the western Mojave Desert. It was among the suite of test rocks and soils used in the development of the 2007–2008 Phoenix Scout and the 2009 Mars Science Laboratory missions [23]. The MRS contains a variety of particle sizes smaller than 1 mm and its microstructure was characterized using X-ray computed tomography in a recent research [24]. Overall, the MRS has a similar chemical composition to the regolith found on Mars with only some slight variations based on the samples taken during the rover missions on Mars [23].

2.2. Biocementation setup

The reactor used for fabricating biocemented MRS columns and biogrout recirculation flow are shown in Fig. 2A, B. The cylindrical tube used to hold and shape the columns is a clear acrylic tubing that has an internal diameter of 3.8 cm and an outer diameter of 5.1 cm. Each of the cylindrical tubes is 12.7 cm in length with a hole at around 11.4 cm from the bottom used to prevent the overflow of biogrout.

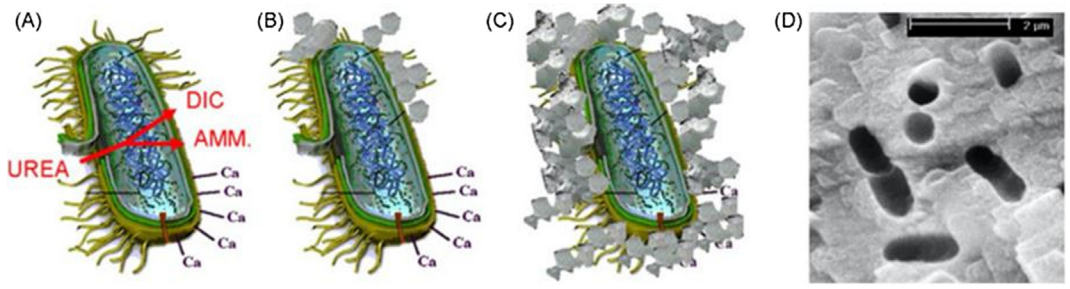

Fig. 1. MICP via urea hydrolysis by urease from UPB [19].

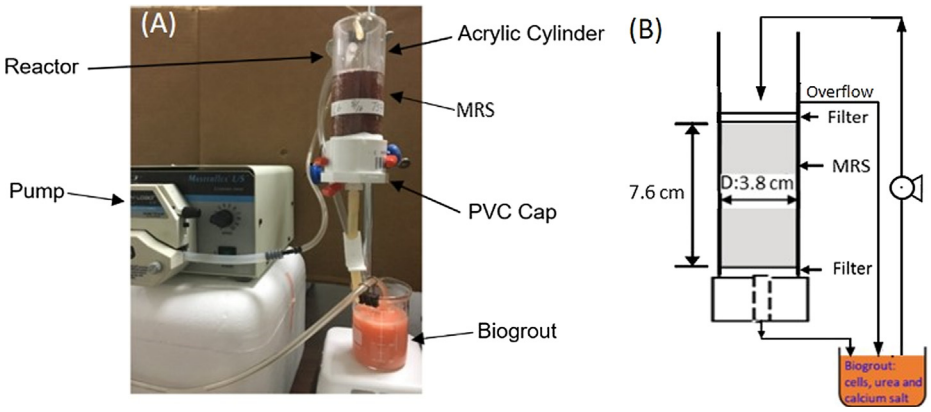

Fig. 2. (A) Biocementation reactor; and (B) biogrout recirculation flow.

All overflowing biogrout collected from the side stream was returned to the 150-mL beaker below the reactor for recirculation. The bottom portion of the reactor was made using a PVC cap that had a hole drilled into the center for barbed hose fitting. A piece of tubing was attached to the fitting to help with the drainage of the reactor back into the beaker below.

Between the bottle cap and the cylindrical tube was a nylon (40 mesh) filter used to help prevent the loss of regolith. A piece of wax paper (15 cm × 9 cm) was attached along the wall inside of the reactor to help with the removal of the columns from the tube at the end of biocementation process. To make columns, each reactor was filled with 105 g of Martian regolith which was rinsed with 150 mL of DDI water to completely wet the regolith and facilitate the uniform distribution of biogrout during the biogrout recirculation. On the top of the regolith is a piece of Scotch-Brite scour pad as a filter to aid in distributing the biomass evenly on top of the regolith. To implement the MICP process, the biogrout was placed in a beaker below the tube and recirculated through a peristaltic pump to the top of the regolith column (Fig. 2). The pumping rate was controlled at a constant of 8.0 mL/min. At the end of a whole biocementation process, the columns were drained of any remaining liquid. The reactors were then flipped upside down in a plastic container to remove the bottom PVC cap. After the columns were air dried upside down for 20 min, they were then flipped back upward and were removed from the tube followed by being placed in the oven to dry overnight at 60 °C. The finished dry columns with dimensions of 3.8 cm (diameter) by 7.6 cm (height) were subject to UCS measurement, hydraulic conductivity measurement, X-ray diffraction (XRD) analysis, and scanning electron microscope (SEM) imaging.

2.3. Variations of biogrouting methods

In contrast to grout formed with conventional cement, biogrout is made from biocementation cells, calcium salt and urea. Many factors were found to significantly impact the properties of biocemented columns, such as sand grain/grout mixing method, calcium salt source/concentration, urea concentration, sand type/-size, cell loading, and so on [3,4,6,10,25]. In this research, we focused on biogrouting method (i.e., how to mix biogrout with MRS in the reactor shown in Fig. 2), calcium salt/urea ratio (Section 2.4) and calcium source ($CaCl_2$ vs. calcium acetate) (Section 2.5). The developed biogrouting methods in this research followed the main biogrouting method of injection, utilizing gravity to aid in the distribution of the microorganisms and nutrients through the pore spaces of the MRS columns [3,5].

Different biogrouting methods including simultaneous feeding, sequential feeding, and batch feeding (coded SIF, SEF and BF, respectively) were developed depending on the recirculation sequence of cell biomass/$CaCl_2$/urea through the MRS columns, the cycle of biogrout recirculation and post-biogrouting soaking time (Fig. 3, Table 1). The purposes to test the sequence are to control the growth/distribution/attachment of cells inside the columns, the urease activity and urea hydrolysis rate to guarantee the occurrence of most urea hydrolysis and $CaCO_3$ precipitation inside the columns and the uniform distribution of cells and $CaCO_3$ precipitation throughout the columns. In different biogrouting methods, we also tested the effect of the post-biogrouting soaking on the properties of biocemented MRS columns given that the urease production rate/activity of *T. striatum* may be slow/low and cells trapped in the column would need a certain amount of time after biogrout recirculation to generate sufficient urease and $CaCO_3$ precipitate.

All biogrouting methods, unless otherwise stated, utilized 2.9 g of *T. striatum* cell biomass (dry basis), 7.2 g of $CaCl_2$, and 17.64 g of urea in total for the production of the biocemented MRS columns. For SIF, the cell biomass and $CaCl_2$/Urea were simultaneously mixed in the beaker and recirculated through the MRS columns for 48 h (Fig. 3). Then, the columns were finally soaked for 0 (i.e. without soaking: the remaining liquid was drained out right away and columns were collected and prepared for property analysis) and 4 d. In SEF, cell biomass and $CaCl_2$/Urea were sequentially added into columns (Fig. 3). Two variables were critical here. The first variable was the time at which $CaCl_2$/urea was added into the circulation stream after the cell biomass was initially recirculated in the column for 3, 6, 9, or 12 h. The total circulation time for both cell biomass and $CaCl_2$/urea was kept constant of 48 h. The second variable was the post-biogrouting soaking time (0, 2, and 4 d).

In addition to SIF and SEF, five different versions of the BF of biogrout were also developed for comparison (Fig. 3 and Table 1). The BFv1 involved a 3-d period of feeding fresh cell mass and $CaCl_2$/urea into the reactor each day. The total amount of cell mass (2.9 g) was evenly distributed over a span of 3 d, with each day being fed with 0.96 g of fresh cell mass. Half of the daily amount of cell mass (0.48 g) was added first into the reactors and circulated within the reactor for 3 h. Following the 3 h, the other half of the daily amount of cell mass was added into the circulation stream along with one-third of the total $CaCl_2$/urea (2.4 g/5.88 g) for 21 h. Once the 3-d of circulation had finished, the columns were soaked for another 3 d. The BFv2 was the same as the first, except that the full amount of the daily fresh cell mass (0.96 g) was added at the beginning of circulation for 3 h followed by $CaCl_2$/urea circulation (no cell biomass) through the columns. The BFv3 was similar to the first version but was conducted over a 2-d period instead of a 3-d period for biogrout recirculation, with a soaking time of 0 and 3 d. In BFv4, the cell mass was harvested by centrifugation, washed and re-suspended in DDI water (removing the effect of media) to produce the biogrout for biocementation. Half of the total daily amount (0.9 g) of cell mass was added at the beginning (0.45 g) and recirculated through the columns for 3 h and the other half was added with one-fifth of the total $CaCl_2$/urea (1.44 g/3.53 g) into the biogrout for a 21-h period of recirculation. The process of biogrout recirculation continued until the columns were clogged and the dripping at the bottom of the reactor had ceased. The BFv5 was the same as BFv4, but the cell mass was not removed from the growth media, i.e., the biogrout for the BFv5 consisted of cells and spent growth media instead of cells and DDI water.

2.4. Influence of $CaCl_2$/urea molar ratio on the properties of MRS columns

Since it produced the strongest columns in the shortest amount of time, the operation procedure for the biogrouting method BFv3 without post-biogrouting soaking (see Table 1) was designated as standard operation procedure (SOP) for this study to determine the effect of $CaCl_2$/urea molar ratio on the UCS of the biocemented MRS columns. Two loadings of $CaCl_2$, i.e., 7.2 and 17.64 g, were used to produce the columns, which was expected to help develop an understanding of the possible effect of $CaCl_2$ on the growth of *T. striatum* [26,27]. Each of the loadings was tested with a set of molar ratios of $CaCl_2$/urea, which included 1:1, 1:4.5, and 1:6 for columns produced with 7.2 g of $CaCl_2$; and 1:1, 1:2, and 1:3 for columns produced with 17.64 g of $CaCl_2$ (summarized in Table 2). The UCS of the biocemented MRS columns and the contents of $CaCO_3$ precipitate within columns were determined for different $CaCl_2$/urea molar ratios.

2.5. Replacement of $CaCl_2$ with simulated AD VFAs-derived calcium acetate

Based on the research of Lim et al. [28] and Wang et al. [29], AD can utilize food waste to produce 24.5–25.5 g COD/L of VFAs with 80% of the VFAs in the form of acetic acid which is equivalent to 18.52 g/L of acetic acid. Thus, pure acetic acid was used to simulate the VFAs produced during the AD of food waste. Utilized to simulate Martian rocks was Espoma Organic Garden Lime, a dolomitic limestone with a calcium carbonate content of around 50%. To solubilize $CaCO_3$ in the limestone to make calcium acetate solution, the dolomitic limestone was soaked in the acetic acid solution for 24 h with agitation at 700 rpm. After 24 h, the solution was filtered to remove any remaining solids and the filtrate was collected as calcium salt solution for making biogrout. To estimate the calcium ion concentration in the prepared filtrate, sodium bicarbonate was added into an aliquot of filtrate to induce the precipitation of calcium within the solution until no precipitation occurred. The suspension was then filtered and the filter paper with retentate solids was collected and dried in the oven overnight at 60 °C. Then, the calcium ion con-

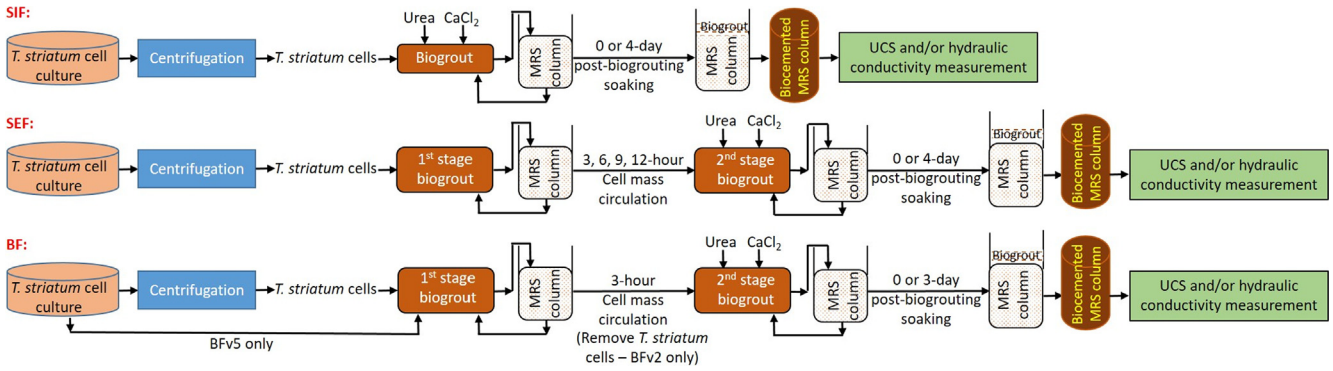

Fig. 3. Schematic of biogrouting methods.

Table 1
Biogrouting methods with specific operation procedures/conditions.

Biogrouting method[a]	Cell mass circulation time (h)	Cell mass (g) circulation		$CaCl_2$/urea circulation time (h)	$CaCl_2$/urea (g) mass circulation		Number of recirculation cycle	Post-biogrouting soaking time (Day)
		Before	After		Before	After		
SIF	0	2.9	0	48	7.2/17.64	0	1	0 & 4
SEF	3	2.9	0	45	0	7.2/17.64	1	0, 2 & 4
SEF	6	2.9	0	42	0	7.2/17.64	1	0 & 4
SEF	9	2.9	0	39	0	7.2/17.64	1	0 & 4
SEF	12	2.9	0	36	0	7.2/17.64	1	0 & 4
BFv1	3	0.48	0.48	21	0	2.4/5.88	3	3
BFv2	3	0.96	0	21	0	2.4/5.88	3	3
BFv3[b]	3	0.73	0.73	21	0	3.6/8.82	2	0 & 3
BFv4	3	0.45	0.45	21	0	1.44/3.53	∞[c]	0
BFv5	3	0.45	0.45	21	0	1.44/3.53	∞	0

[a] SIF = simultaneous feeding, SEF = sequential feeding and BFv# = batch feeding version #.
[b] BFv3 without soaking time (i.e., 0 day) was selected as the standard operation procedure (SOP) since it achieved the best UCS.
[c] Until flow through column stops, i.e., columns were clogged.

Table 2
Varying $CaCl_2$/urea molar ratios in SOP.

Biogrouting method[a]	Cell mass circulation time (h)	Cell mass circulation (g)		Total $CaCl_2$ (g)	$CaCl_2$/urea circulation time (h)	$CaCl_2$/urea (g/g)	Number of recirculation cycle
		Before	After				
SOP (1:1)	3	0.73	0.73	7.2 17.64	21 21	3.60/1.95 8.82/3.60	2
SOP (1:2)	3	0.73	0.73	17.64	21	8.82/7.20	2
SOP (1:3)	3	0.73	0.73	17.64	21	8.82/10.8	2
SOP (1:4.5)	3	0.73	0.73	7.2	21	3.60/8.82	2
SOP (1:6)	3	0.73	0.73	7.2	21	3.60/11.7	2

[a] SOP (#:#) = Standard Operation Procedure ($CaCl_2$:urea molar ratio) from BFv3 without post-biogrouting soaking (Table 1).

centration can be estimated based on the consumption of sodium bicarbonate and precipitated calcium carbonate. The optimum ratio of limestone to acetic acid solution (20 g per 100 mL) was determined by following the aforementioned procedures. The SOP (i.e., BFv3 without post-biogrouting soaking) was used as the biogrouting method for this study, while calcium acetate was used to replace $CaCl_2$ as a calcium ion source for comparison. The columns were produced utilizing three different molar ratios of calcium acetate (7.2 g) to urea such as 1:0, 1:1, and 1:4.5. The produced biocemented MRS columns were subjected to UCS measurements, hydraulic conductivity measurements, XRD analysis, and carbonate quantification.

2.6. Characterization and testing methods

The UCS of the biocemented MRS columns was measured by following the ASTM C39 standard method [30]. The columns had a 1:2 diameter-to-height ratio, and the standard suggests a loading rate which corresponded to a stress rate of 0.25 ± 0.05 MPa/s on the columns. However, following this stress rate the biocemented columns would be crushed in a few seconds due to their relatively lower strength compared to conventional concrete. Therefore, this test used a deformation driven scheme to apply the axial compressive load at a constant rate of 1.0 mm/min [31] for testing biocemented MRS columns. This loading rate produces a strain rate of about 1.3%/min, which allows for the columns to break within a 2-min time period. The measurement of the hydraulic conductivity followed the ASTM D5856 standard method [32], which includes a falling head permeability test utilized to characterize the water permeability of the biocemented MRS columns. Prior to the test, DDI water was flushed through the permeameter to remove any entrapped gases with a pressure of about 10 kPa. Once the influent pressure was stabilized to about 10 kPa and the effluent pressure was stabilized to atmospheric pressure, then DDI water was allowed to flow through the column due to the pressure difference while the time and head loss were recorded.

XRD analysis was utilized to determine the presence of $CaCO_3$ and identify the type of $CaCO_3$ precipitated within the biocemented MRS columns. Upon completion of the UCS test, the broken column was separated into different sections (top, middle and bottom) of the columns. XRD scans were conducted on each of the sections. Before the biocemented regolith was scanned, it was further pulverized making the samples a fine powder with the use of a mortar and pestle. The instrument parameters used to run these scans were similar to those used by Wei et al. [18] with some slight adjustments. The accelerating voltage and current were set to 40 kV

and 35 mA, respectively. The samples were scanned from 20 to 40° (2θ) with a scanning speed of one degree per min. SEM imaging was utilized to visualize the precipitation of $CaCO_3$. Similar to XRD, the different sections of the broken columns from the UCS tests were scanned for the confirmation of $CaCO_3$. The samples were prepared by placing a small piece of the biocemented MRS column coated in platinum onto the sample tray. After venting the SEM, the tray was placed within the chamber and the chamber was sealed via vacuum pumping. The sample was scanned using the SE detector and the beam voltage was set to 3.0 kV. The spot size, contrast and brightness were adjusted for better picture quality. The scanned photographs were taken with a resolution of 5, 10, 20, 30, 100, 200, and 500 μm.

The carbonate quantification via titration was used to determine the amount of $CaCO_3$ (%, wt/wt) deposited within the columns during biocementation [33]. After the UCS measurement, the broken columns were also used for $CaCO_3$ quantification besides XRD analysis and SEM imaging. Each biocementation condition was conducted in triplicate in this research unless specified, otherwise.

3. Results and discussion

3.1. Confirmation of MICP via XRD and SEM

Both untreated and biocemented MRS were analyzed by using XRD and SEM to detect the $CaCO_3$ precipitate during MICP and observe the microstructure of columns, respectively. The representative biocemented MRS columns used for such analyses were produced using SEF biogrouting method with 3-h cell mass circulation but without soaking (Table 1). The XRD patterns found in the biocemented MRS columns (Fig. 4A) matched those of the pure reagent grade of $CaCO_3$ as calcite (Fig. 4B) and aragonite (Fig. 4C). The distribution of $CaCO_3$ within the columns was fairly even throughout from top to bottom. There were some cases where one section was slightly higher in $CaCO_3$ than the other sections, but for the most part, these sections were only off by a small amount.

The microstructure of the biocemented columns obtained by SEM imaging is shown in Fig. 5. After the biocementation treatment, MRS particle surfaces were covered by $CaCO_3$ crystals compared to the untreated MRS particles (Fig. 5A, B). In other areas of the biocemented regolith columns, there were deposits of aragonite on the MRS particles (Fig. 5C). The deposits of aragonite crystals within the biocemented MRS columns were further verified through the XRD analysis (Fig. 4C). The polymorphs of the $CaCO_3$ crystal deposits depends on the type of biocementation microorganism, calcium source, and sand type [34,35]. Further studies will be needed to study the formation of $CaCO_3$ polymorphs in different MICP processes and the relationship between the polymorphs and properties of MRS columns.

The results of the SEM imaging has shown that $CaCO_3$ crystals were formed and the majority of $CaCO_3$ was uniformly distributed on the MRS particle surfaces (Fig. 5A–C). Though a few locations within the SEM images (Fig. 5B, C) had shown that $CaCO_3$ precipitated within the pore spaces creating a connection between two different MRS particle surfaces (i.e., localized distribution). The distribution of precipitated $CaCO_3$ on the MRS particle surfaces was a by-product of the biogrouting [3,5]. When comparing uniform and localized distributions, it has been determined that localized distributions have led to an increase in the strength of biocemented regolith [3,5]. This increase in strength is due to the increase in points of contact between different particle surfaces [3,5]. Though the type of $CaCO_3$ distribution seen in the SEM images (Fig. 5B, C) were not favorable, this was only a small section of the biocemented MRS column and is not fully indicative of the entire column. Since the precipitation of $CaCO_3$ throughout the column is just as important as the type of distribution [3,5,13,14].

3.2. Effect of biogrouting methods on UCS of biocemented MRS columns

The time, quantity and sequence of circulation of cells, calcium salt and urea can affect the amount, generation rate, distribution of $CaCO_3$ precipitate and eventually UCS [3,5]. In addition, the post-biogrouting soaking of columns was expected to enhance the UCS due to the biocementation resulted from the trapped cells. Therefore, we comprehensively studied the impact of biogrouting methods including soaking on the mechanical property of MRS columns. As shown in Table 3, the UCS of columns from SEF is higher than that from SIF with the same soaking time. This result may be because SEF allowed sufficient time for *T. striatum* cells to generate $CaCO_3$ gradually inside the columns, while the cells produced $CaCO_3$ too fast in SIF and left a large amount of $CaCO_3$ outside

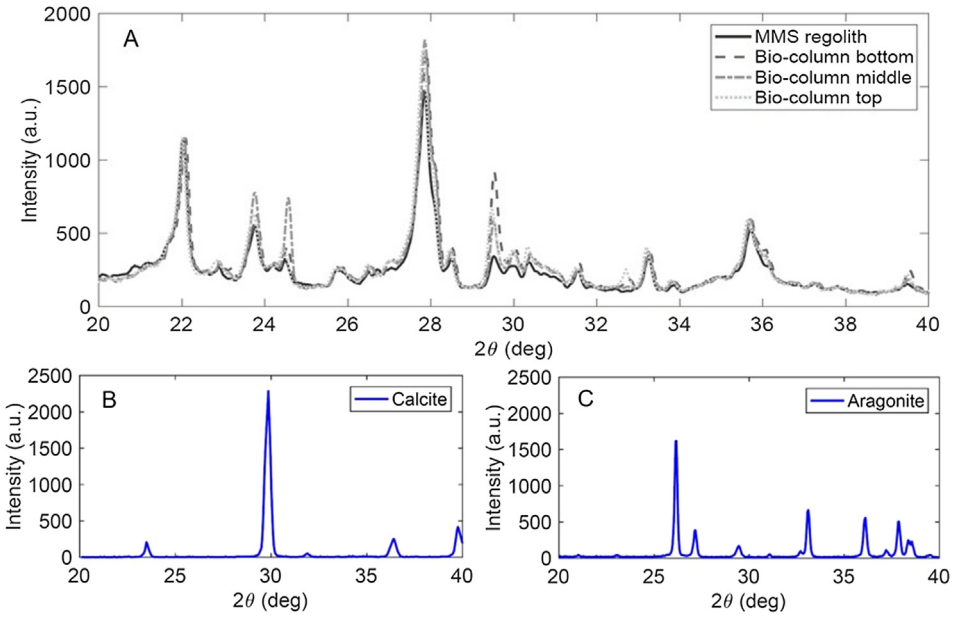

Fig. 4. (A) XRD spectra of the untreated MRS regolith and biocemented MRS at different locations in the columns, (B) the pure reagent grade $CaCO_3$ as calcite, and (C) the aragonite standard. "Bio-column" within the legend represents the biocemented MRS columns, and MRS means untreated Martian regolith simulant.

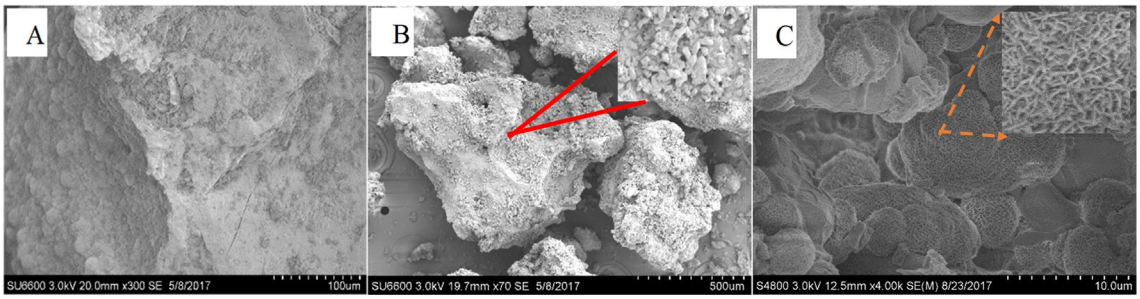

Fig. 5. SEM images of untreated and biocemented MRS: (A) untreated MRS particles; (B) calcite crystals attached to the particle surface and a zoom-in view of calcite crystals (the inset), and (C) aragonite crystals attached on the particle surface and a zoom-in view of aragonite crystals (the inset).

Table 3
Comparison of SIF with SEF methods and effect of post-biogrouting soaking on UCS (mean ± standard deviation) based on triplicate MRS columns.

Cell mass circulation time for different biogrouting methods (h)	Post-biogrouting soaking time (Day)	UCS (kPa)
0 (SIF)	0	365.96 ± 44.25
	4	199.4 ± 88.06
3 (3-h SEF)	0	508.24 ± 83.07
	2	453.18 ± 144.24
	4	268.01 ± 136.72
6 (6-h SEF)	0	472.67 ± 72.64
	4	337.20 ± 156.91
9 (9-h SEF)	0	385.93 ± 35.72
	4	221.72 ± 45.21
12 (12-h SEF)	0	408.84 ± 85.06
	4	159.34 ± 62.23

Table 4
Effect of BF biogrout recirculation method on UCS.

Version	Soaking time (Day)	UCS (kPa)
BFv1	3	290.43 ± 46.10
BFv2	3	179.81 ± 54.62
BFv3	0	732.40 ± 117.84
	3	538.58 ± 210.04
BFv4	0	728.99 ± 106.17
BFv5	0	468.09 ± 123.42

the columns (top and bottom of columns and/or in the beaker containing biogrout) during biogrouting [35]. This phenomenon was visually observed during experiments. The investigation of post-biogrouting soaking showed that soaking reduced UCS of biocemented MRS columns. For instance, the UCS of the biocemented MRS columns made from 3-h SEF decreased about 2 folds from 508 to 268 kPa as the soaking time increased from 0 to 4 h (Table 3). Similar results were also obtained for SIF and other SEF scenarios, i.e., the UCS of the columns on average without soaking is about twice as strong as that of the columns soaked for a period of 4 days.

As also shown in Table 3, the increase of cell mass circulation time led to decreasing UCS under the same post-biogrouting soaking time. The optimum cell circulation time before the addition of $CaCl_2$/urea to the biogrout was 3 h, which could give the cells sufficient time to penetrate and distribute uniformly inside the MRS columns before secreting urease for precipitating $CaCO_3$ inside the columns, resulting in higher UCS of MRS columns.

In addition to biogrouting methods of SIF and SEF, five different versions of BF with and without soaking were also tested. The comparison between BFv1 and BFv2 showed that completely separating the cell mass circulation from the $CaCl_2$/urea circulation in sequence led to a significant decrease in the UCS from 290 (BFv1) to 179 (BFv2) kPa even though both versions had the same total cell mass in the biogrout (Table 4). In BFv1, it was found that a large amount of $CaCO_3$ precipitation occurred in the beaker and on the top of the column, which clogged the column and reduced the $CaCO_3$ formation inside the column, resulting in low UCS. This clogging could be owing to the excessive urease activity, which made $CaCO_3$ precipitation occur too fast outside the columns during biogrout recirculation [35]. However, much less $CaCO_3$ precipitation occurred in BFv2, which could indicate cells did not produce sufficient urease with the BFv2 biogrouting method. To mitigate the clogging problem, in BFv3, the daily amount of cell mass and $CaCl_2$/urea in each circulation were increased while the biogrout circulation time was reduced to 2 d. In doing so, the BFv3 achieved double UCS of the columns compared to BFv1 (Table 4). The increase in strength of columns could be due to the increased cell mass distribution within the columns because higher cell mass and urease activity stayed inside the columns compared to BFv1 [3,5,13,14]. This allowed for fresher cells to grow by using $CaCl_2$/urea that was added after the 3-h cell mass circulation, which in turn led to a better distribution of cells and $CaCO_3$ precipitate throughout the columns as well as higher UCS.

Similar to SIF and SEF, no post-biogrouting soaking in BFv3 resulted in higher UCS when compared to 3-d soaking. During biogrouting, we found the biogrout recirculation completed (i.e., columns got clogged) in BFv5, one day earlier than that in BFv4 even though both biogrouting methods used the same amount of cell mass and $CaCl_2$/urea each day. It was discovered that the biocemented MRS columns produced from BFv5 had lower UCS than those from BFv4 (Table 4). The decrease in UCS may be attributed to the salts and/or extracellular polymeric substances (EPSs) within the growth media in BFv5 blocking the pore spaces which would normally be occupied by the cells; this could also be the reason why biogrout recirculation stopped a day earlier for BFv5 than BFv4 [6]. Another possibility is that cells grew faster with growth medium in BFv5 than with DDI water in BFv4 during biogrouting so that the columns in BFv5 were clogged by cells quickly and the produced $CaCO_3$ did not distribute well inside the columns [3,35].

With the comparison among the SIF, SEF and BF, BF appeared to be the best biogrouting method to generate the strongest MRS columns. This could be attributed to the type of distribution (Section 3.1) and placement of $CaCO_3$ within the column from utilizing the BF method of biogrouting [3,5,13,14]. Although both BFv3 (no soaking) and BFv4 achieved similar UCS of the biocemented MRS columns which were much higher than columns made with all other tested biogrouting methods (Tables 3, 4), BFv4 used 5 days compared to 2 days for BFv3. Therefore, the procedure of BFv3 without soaking was selected as an SOP for subsequent biocementation studies on effects of $CaCl_2$/urea molar ratio and alternative calcium source.

3.3. Effect of $CaCl_2$/urea molar ratio on $CaCO_3$ precipitate and UCS of biocemented MRS columns

The measurement of the $CaCO_3$ content inside the biocemented MRS columns produced from the SOP with $CaCl_2$ loading of 17.64 g showed that the average content of $CaCO_3$ precipitate increased from 12.05 to 12.69% with the decrease of $CaCl_2$/urea molar ratio from 1:1 to 1:3 (Fig. 6A). By measuring the contents of $CaCO_3$ throughout the columns, it was found that the $CaCO_3$ precipitate distribution inside the columns during biocementation varied significantly. Taking the columns with $CaCl_2$/urea = 1:1 as an example, the top portion of the columns contained 12.50% $CaCO_3$ in average, whereas the average $CaCO_3$ content of the bottom portion of the columns was 12.25%. The $CaCO_3$ content in the middle portions of the columns had much more variance. This may be attributed to the random distribution of the MRS grains of varied size within the columns, which affected the flow of the biogrout through the columns and further affected the distribution of cells, $CaCl_2$ and/or urea within the columns. The biogrout flow affected by the middle portion of the columns could possibly dictate the distribution of $CaCO_3$ precipitate within the biocemented MRS columns, which will need to be further studied. While investigating the relationship between the UCS and $CaCO_3$ content (or $CaCl_2$/urea molar ratio) of the biocemented MRS columns, we found an unexpected result that the increase of $CaCO_3$ content (or decrease of $CaCl_2$/urea molar ratio) reduced the UCS of columns (Fig. 6A).

Upon reducing the $CaCl_2$ loading to 7.2 g, both $CaCO_3$ content and UCS increased with the increase of the $CaCl_2$/urea ratio and peaked at the ratio of 1:4.5, then decreased when the ratio further increased to 1:6 (Fig. 6B). This result could be caused by urea inhibition that reduced urease activity for urea hydrolysis, resulting in low content of $CaCO_3$ precipitate and low UCS of columns [26,27]. In addition, it can be seen that the UCS of the columns made with 17.64 g of $CaCl_2$ were much lower than that of the columns made with 7.2 g $CaCl_2$ at the same $CaCl_2$/urea molar ratio (Fig. 6A, B). It was found that the pH of the former system, measured from the biogrout in the beakers, stayed at around 7.0 after the first and second day of circulation. The stable pH of the system could be due to the inhibition of *T. striatum* by the high concentration of $CaCl_2$ [26,27], leading to low urease activity for urea hydrolysis which caused low $CaCO_3$ precipitate inside the columns (Fig. 6A). Whereas, the pH of the biogrout made from 7.2 g $CaCl_2$ increased with the increase of urea (i.e., decreased $CaCl_2$/urea ratio). The pH of the system, measured from the biogrout in the beakers, was 7.0 after the first day of biogrout circulation and increased to 8–9 after the second day of circulation. This could indicate that the increase in urea led to an increase in urease production and urea hydrolysis resulting in an increase in the pH of the system, which resulted in more $CaCO_3$ precipitate and higher UCS of columns [3,10,35].

3.4. Study of alternative calcium source from simulated AD VFAs-derived calcium acetate for biocementation of MRS

3.4.1. Confirmation of MICP via XRD

Simulated AD VFAs-derived calcium acetate was used to replace $CaCl_2$ to make biocemented MRS columns with and without urea using the SOP biogrouting method, and XRD was used to detect the $CaCO_3$ precipitate inside the columns. Overall, similar to the XRD results of the columns produced with $CaCl_2$ (Fig. 4), there was calcite detected at 29–30° (2θ) (Fig. 7). As expected, *T. striatum* was able to generate $CaCO_3$ precipitate from calcium acetate metabolism in the absence of urea through the pathway that acetate is degraded into CO_3^{2-} which forms $CaCO_3$ with Ca^{2+}. In this process, calcium acetate plays dual roles of organic carbon and calcium sources. Therefore, the utilization of acetate from the simulated AD of food waste as a carbon/calcium source to produce carbonate without urea can avoid the issue of ammonia emission associated with the conventional MICP using UPB. This is the first report about biocementation using microalga and calcium acetate to form biogrout without urea, which is worth being further researched. Another idea deduced from this result would be using anaerobic degradation of acetate to produce carbonate for biocementation for space application.

3.4.2. Effect of calcium acetate/urea molar ratio on UCS and $CaCO_3$ content of columns

Overall, the UCS of the columns produced utilizing calcium acetate were lower (Fig. 8) than that of the columns manufactured with $CaCl_2$ (Fig. 6B) with the same calcium salt loading of 7.2 g. During the production of columns utilizing 1:4.5 of calcium acetate/urea molar ratio, it was noticed that by the end of the first day there was a large amount of $CaCO_3$ precipitated on top of the Scotch-Brite scour pad and within the beaker containing the biogrout instead of inside the column. This phenomenon indicated that the cells generated a significant amount of urease due to a high urea loading, resulting in a rapid urea hydrolysis and $CaCO_3$ precipitation outside the columns [35]. As for the columns produced without urea, all columns collapsed after 30 min after being removed from the reactors, which may be attributed to the placement of the precipitated $CaCO_3$, given little numerical difference was found in the average $CaCO_3$ content throughout the columns compared to the other molar ratios (Fig. 8) [3,5,13,14]. Thus, the $CaCO_3$ content inside the columns derived from biocementation may not be a main determining factor for UCS.

Upon a further look into the distribution of $CaCO_3$ content within the different layers of the columns, it can be seen that all columns that share a similar pattern of $CaCO_3$ distribution have a discrepancy in UCS (Fig. 9). This may be ascribed to the small discrepancy of $CaCO_3$ content between different layers. Considering results from both Fig. 8 and Fig. 9, we could deduce that the distri-

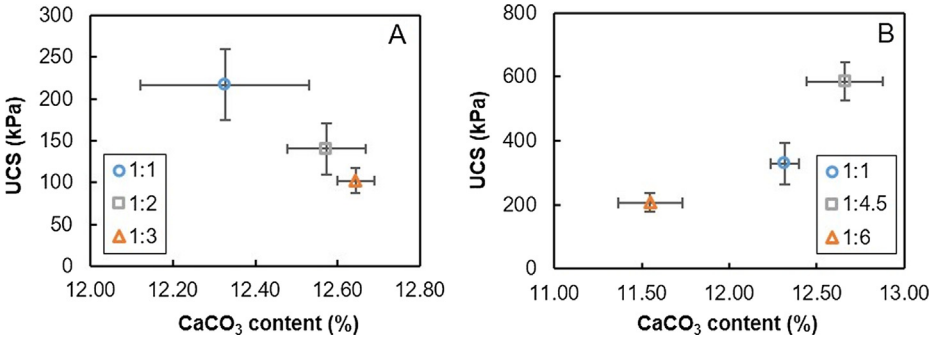

Fig. 6. Effect of $CaCl_2$/urea molar ratio on the content of $CaCO_3$ precipitate and the UCS of the columns. (A) Columns with 17.64 g of $CaCl_2$ and (B) Columns with 7.2 g of $CaCl_2$. #:# within the legend represents $CaCl_2$/urea molar ratio.

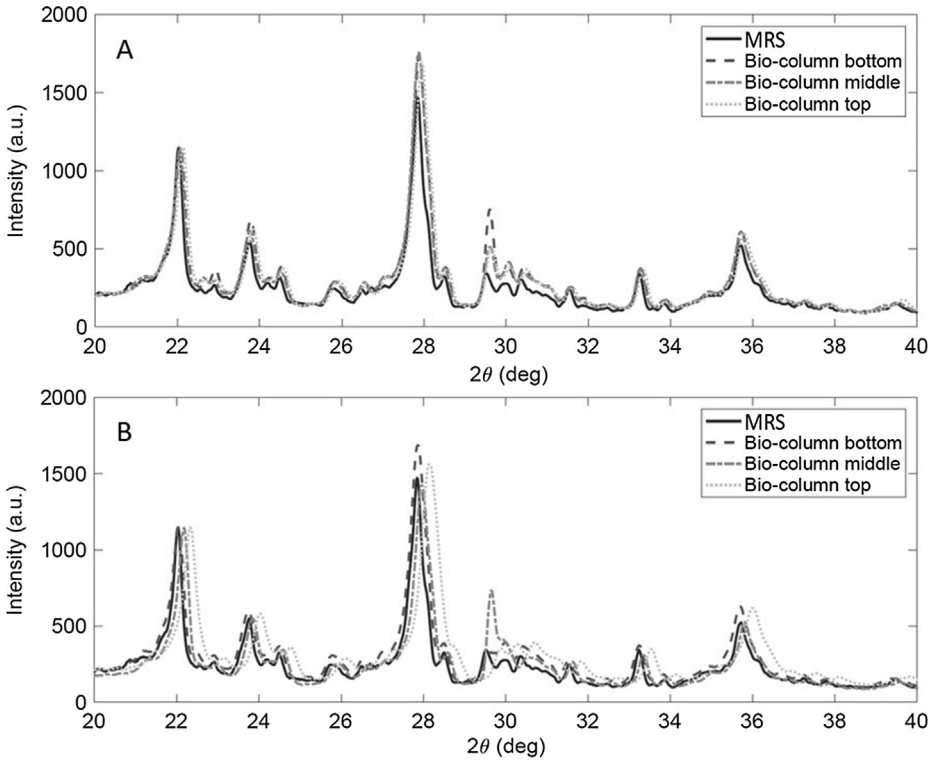

Fig. 7. XRD spectra of biocemented columns using simulated AD VFAs-derived calcium acetate with (A) and without urea (B). "Bio-column" within the legends represents the biocemented MRS columns produced with SOP biogrouting method while "MRS" represents the untreated MRS.

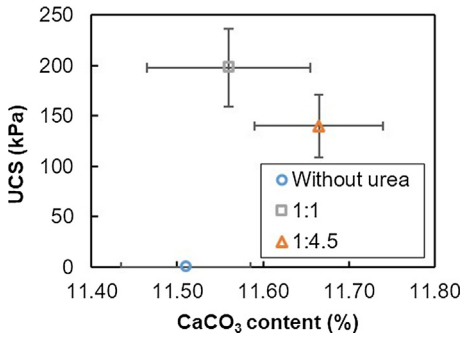

Fig. 8. Effect of calcium acetate/urea molar ratio on the content of $CaCO_3$ precipitate and the UCS of the columns with 7.2 g of simulated AD VFAs-derived calcium acetate. #:# within the legend represents calcium acetate/urea molar ratio.

bution of $CaCO_3$ precipitate within the columns play a more significant role than the total amount of $CaCO_3$ content of columns in affecting the column UCS [13,14]. In addition, the number/distribution of cells in the columns, the polymorph of formed $CaCO_3$ and/or the microstructure of the MRS columns in the reactors could be other possible reasons for this effect on the UCS [3,5,13,14]. Therefore, further research will need to be conducted to identify the determining factors that affect the UCS of the columns.

3.4.3. Effects of calcium source and calcium acetate/urea molar ratio on hydraulic conductivity of columns

The hydraulic conductivities of untreated MRS and biocemented MRS columns with $CaCl_2$ and simulated AD VFAs-derived calcium acetate are shown in Fig. 10. Biocementation with $CaCl_2$ reduced about 50% of hydraulic conductivity compared to the untreated MRS, while more than 95% reduction of hydraulic conductivity was achieved with calcium acetate (Fig. 10). Although

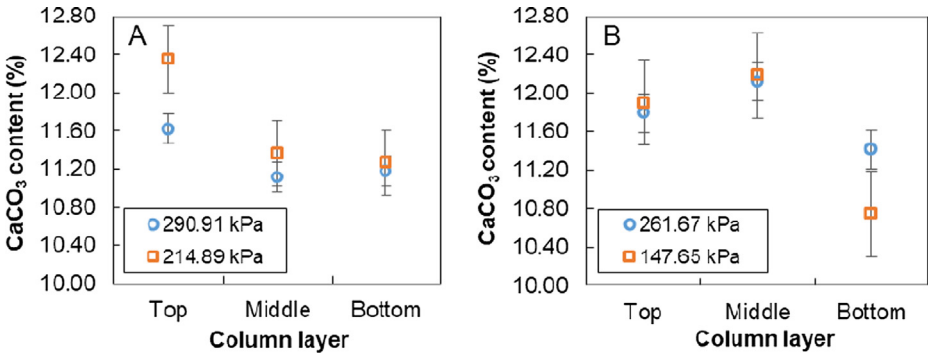

Fig. 9. Effect of calcium acetate/urea molar ratio (A) 1:1 and (B) 1:4.5 on $CaCO_3$ content at different layers of columns with different UCS.

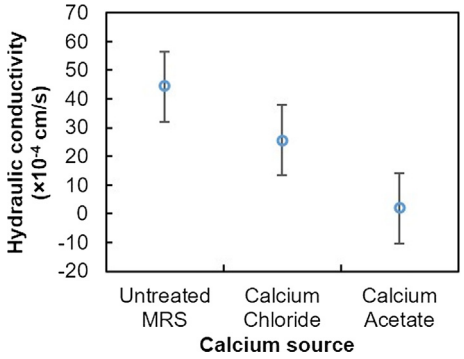

Fig. 10. Comparison of hydraulic conductivity among biocemented columns produced with $CaCl_2$ and calcium acetate with a molar ratio of calcium salt/urea = 1:4.5.

the content of $CaCO_3$ precipitate and UCS of calcium acetate-based biocemented MRS columns were less than that of the columns made from $CaCl_2$ (Figs. 6B and 8), the hydraulic conductivity of calcium acetate-based columns was much lower than that of $CaCl_2$-based columns. Thus, we can't ascribe such results just to the content of $CaCO_3$ precipitate from MICP. Other reasons could be the internal structure of the columns, the polymorph of $CaCO_3$ precipitate formed by different calcium sources and/or any remaining unused calcium acetate [3,5,13,14]. Further studies will need to be conducted to clarify this phenomenon by finding the exact relationship among UCS, the hydraulic conductivity of columns, the internal microstructure of MRS columns, and $CaCO_3$ formation (e.g., content, polymorph and distribution).

4. Conclusions

Microalga, *T. striatum* is capable of being used to make biocementation of MRS. In the presence of $CaCl_2$ and urea, *T. striatum* generated $CaCO_3$ through urease activity in the form of calcite and aragonite on the surface of the MRS grains. The biogrouting method of BFv3 without post-biogrout soaking (SOP) produced the strongest MRS columns with an average UCS of 732.40 kPa. The hydraulic conductivity of the SOP columns was 2.56×10^{-3} cm/s, which was 50% less than the untreated MRS. The utilization of simulated AD VFAs-derived calcium acetate caused a significant decrease in the hydraulic conductivity by 95% compared to the untreated MRS. Overall, *T. stratum* was able to utilize calcium acetate as both carbon and calcium source to precipitate carbonate. AD could be an effective way to generate an inexpensive alternative calcium source for biocementation in replacement of conventionally used $CaCl_2$. Further research will be needed to enhance and optimize the biocementation with *T. striatum* and AD-derived calcium source and investigate possible applications for space exploratory missions.

Declaration of Competing Interest

None.

Acknowledgements

This work was supported by the National Aeronautics and Space Administration (NASA) of the United States through South Carolina Space Consortium Grants (Grant numbers NNX15AK53A and NNX15AL49H, 2016, 2017).

References

[1] D. Ariyanti, N. Abyor Handayani, An overview of biocement production from microalgae, Int. J. Sci. Eng. Dessy Ariyanti Al. 2 (2011) 30–33, https://doi.org/10.12777/ijse.2.2.31-33.
[2] D. Ariyanti, N.A. Handayani, Feasibility of using microalgae for biocement production through, Bioprocess. Biotech. 2 (2012) 8–11, https://doi.org/10.4172/2155-9821.1000111.
[3] D. Mujah, M.A. Shahin, L. Cheng, State-of-the-art review of biocementation by microbially induced calcite precipitation (MICP) for soil stabilization, Geomicrobiol J. 34 (2017) 524–537, https://doi.org/10.1080/01490451.2016.1225866.
[4] S.G. Choi, J. Chu, R.C. Brown, K. Wang, Z. Wen, Sustainable biocement production via microbially induced calcium carbonate precipitation: use of limestone and acetic acid derived from pyrolysis of lignocellulosic biomass, ACS Sustain. Chem. Eng. 5 (2017) 5183–5190, https://doi.org/10.1021/acssuschemeng.7b00521.
[5] A.M. Sharaky, N.S. Mohamed, M.E. Elmashad, N.M. Shredah, Application of microbial biocementation to improve the physico-mechanical properties of sandy soil, Constr. Build. Mater. 190 (2018) 861–869, https://doi.org/10.1016/j.conbuildmat.2018.09.159.
[6] S. Joshi, S. Goyal, M.S. Reddy, Influence of nutrient components of media on structural properties of concrete during biocementation, Constr. Build. Mater. 158 (2018) 601–613, https://doi.org/10.1016/j.conbuildmat.2017.10.055.
[7] G. Kaur, N.K. Dhami, S. Goyal, A. Mukherjee, M.S. Reddy, Utilization of carbon dioxide as an alternative to urea in biocementation, Constr. Build. Mater. 123 (2016) 527–533, https://doi.org/10.1016/j.conbuildmat.2016.07.036.
[8] S.-G. Choi, S.-S. Park, S. Wu, J. Chu, Methods for calcium carbonate content measurement of biocemented soils, J. Mater. Civ. Eng. 29 (2017) 06017015, https://doi.org/10.1061/(asce)mt.1943-5533.0002064.
[9] K. Feng, B.M. Montoya, T.M. Evans, Discrete element method simulations of bio-cemented sands, Comput. Geotech. 85 (2017) 139–150, https://doi.org/10.1016/j.compgeo.2016.12.028.
[10] G. Kim, J. Kim, H. Youn, Effect of Temperature, pH, and Reaction Duration on Microbially Induced Calcite Precipitation, Appl. Sci. 8 (2018) 1277, https://doi.org/10.3390/app8081277.
[11] L. Liu, H. Liu, Y. Xiao, J. Chu, P. Xiao, Y. Wang, Biocementation of calcareous sand using soluble calcium derived from calcareous sand, Bull. Eng. Geol. Environ. 77 (2018) 1781–1791, https://doi.org/10.1007/s10064-017-1106-4.
[12] N.K. Dhami, M.S. Reddy, M.S. Mukherjee, Biomineralization of calcium carbonates and their engineered applications: a review, Front. Microbiol. 4 (2013) 1–13, https://doi.org/10.3389/fmicb.2013.00314.
[13] A. Dadda, C. Geindreau, F. Emeriault, S.R. du Roscoat, A. Garandet, L. Sapin, A.E. Filet, Characterization of microstructural and physical properties changes in biocemented sand using 3D X-ray microtomography, Acta Geotech. 12 (2017) 955–970, https://doi.org/10.1007/s11440-017-0578-5.
[14] A. Dadda, C. Geindreau, F. Emeriault, S. Rolland du Roscoat, A. Esnault Filet, A. Garandet, Characterization of contact properties in biocemented sand using 3D X-ray micro-tomography, Acta Geotech. 14 (2019) 597–613, https://doi.org/10.1007/s11440-018-0744-4.
[15] Varalakshmi, Isolation and characterization of urease utilizing bacteria to produce biocement, IOSR J. Environ. Sci. Ver. II 8 (2014) 2319–2399, https://doi.org/10.9790/2402-08425257.
[16] R.K. Verma, L. Chaurasia, V. Bisht, M. Thakur, Bio-mineralization and bacterial carbonate precipitation in mortar and concrete, Am. Inst. Sci. J. Biosci. Bioeng. 1 (2015) 5–11.
[17] P. Anbu, C.-H. Kang, Y.-J. Shin, J.-S. So, Formations of calcium carbonate minerals by bacteria and its multiple applications, SpringerPlus 5 (1) (2016), https://doi.org/10.1186/s40064-016-1869-2.
[18] S. Wei, H. Cui, Z. Jiang, H. Liu, H. He, N. Fang, Biomineralization processes of calcite induced by bacteria isolated from marine sediments, Brazilian J. Microbiol. 46 (2015) 455–464, https://doi.org/10.1590/S1517-838246220140533.
[19] W. De Muynck, N. De Belie, W. Verstraete, Microbial carbonate precipitation in construction materials: a review, Ecol. Eng. 36 (2010) 118–136, https://doi.org/10.1016/j.ecoleng.2009.02.006.
[20] M.A. Khan, H.H. Ngo, W.S. Guo, Y. Liu, L.D. Nghiem, F.I. Hai, L.J. Deng, J. Wang, Y. Wu, Optimization of process parameters for production of volatile fatty acid, biohydrogen and methane from anaerobic digestion, Bioresour. Technol. 219 (2016) 738–748, https://doi.org/10.1016/j.biortech.2016.08.073.
[21] Y. Zheng, J. Zhao, F. Xu, Y. Li, Pretreatment of lignocellulosic biomass for enhanced biogas production, Prog. Energy Combust. Sci. 42 (2014) 35–53, https://doi.org/10.1016/j.pecs.2014.01.001.
[22] R. Xiao, X. Li, Y. Zheng, Comprehensive study of cultivation conditions and methods on lipid accumulation of a marine protest, thraustochytrium striatum, Protist 169 (2018) 451–465, https://doi.org/10.1016/j.protis.2018.05.005.
[23] G.H. Peters, W. Abbey, G.H. Bearman, G.S. Mungas, J.A. Smith, R.C. Anderson, S. Douglas, L.W. Beegle, Mojave mars simulant-characterization of a new geologic mars analog, Icarus 197 (2008) 470–479, https://doi.org/10.1016/j.icarus.2008.05.004.
[24] Z. Lai, Q. Chen, Reconstructing granular particles from X-ray computed tomography using the TWS machine learning tool and the level set method, Acta Geotech. (2018), https://doi.org/10.1007/s11440-018-0759-x.

[25] A. Al Qabany, K. Soga, C. Santamarina, Factors affecting efficiency of microbially induced calcite precipitation, J. Geotech. Geoenvironmental Eng. 138 (2012) 992–1001, https://doi.org/10.1061/(ASCE)GT.1943-5606.0000666.
[26] J. Bautista-Gallego, F.N. Arroyo-Lopez, M.C. Duran-Quintana, A. Garrido-Fernandez, Individual effects of sodium, potassium, calcium, and magnesium chloride salts on lactobacillus pentosus and saccharomyces cerevisiae growth, J. Food Prot. 71 (2008) 1412–1421, https://doi.org/10.1016/B978-0-12-420067-8.00012-X.
[27] M.X. Vieira Megda, E. Mariano, J.M. Leite, M.M. Megda, P.C. Ocheuze Trivelin, Chloride ion as nitrification inhibitor and its biocidal potential in soils, Soil Biol. Biochem. 72 (2014) 84–87, https://doi.org/10.1016/j.soilbio.2014.01.030.
[28] S.J. Lim, B.J. Kim, C.M. Jeong, J. dal rae Choi, Y.H. Ahn, H.N. Chang, Anaerobic organic acid production of food waste in once-a-day feeding and drawing-off bioreactor, Bioresour. Technol. 99 (2008) 7866–7874, https://doi.org/10.1016/j.biortech.2007.06.028.
[29] K. Wang, J. Yin, D. Shen, N. Li, Anaerobic digestion of food waste for volatile fatty acids (VFAs) production with different types of inoculum: Effect of pH, Bioresour. Technol. 161 (2014) 395–401, https://doi.org/10.1016/j.biortech.2014.03.088.
[30] ASTM C39, Standard Test Method for Compressive Strength of Cylindrical Concrete Specimens, ASTM International, West Conshohocken, PA, 2016. https://doi.org/10.1520/C0039.
[31] L. Cheng, R. Cord-Ruwisch, M.A. Shahin, Cementation of sand soil by microbially induced calcite precipitation at various degrees of saturation, Can. Geotech. J. 50 (2013) 81–90, https://doi.org/10.1139/cgj-2012-0023.
[32] ASTM Standard D5856, Standard Test Method for Measurement of Hydraulic Conductivity of Porous Material Using a Rigid-Wall, Compaction-Mold Permeameter, ASTM International, West Conshohocken, PA, 2015. https://doi/org/10.1520/D5856-15.2.
[33] D.L. Rowell, Soil Science: Methods and Applications, Longman Scientific & Technical, Harlow, 1994.
[34] Y. Zhang, H.X. Guo, X.H. Cheng, Influences of calcium sources on microbially induced carbonate precipitation in porous media S2-79-S2-84, Mater. Res. Innov. 18 (2014), https://doi.org/10.1179/1432891714Z.000000000384.
[35] S.G. Choi, K. Wang, J. Chu, Properties of biocemented, fiber reinforced sand, Constr. Build. Mater. 120 (2016) 623–629, https://doi.org/10.1016/j.conbuildmat.2016.05.124.